GLIA 2:318–329 (1989)

Expression of Viral and Myelin Gene Transcripts in a Murine CNS Demyelinating Disease Caused by a Coronavirus

CRAIG A. JORDAN,[1] VICTOR L. FRIEDRICH, JR.,[1] CATHERINE GODFRAIND,[1] CHRISTINE B. CARDELLECHIO,[2] KATHRYN V. HOLMES,[2] AND MONIQUE DUBOIS-DALCQ[1]
[1]*Laboratory of Viral and Molecular Pathogenesis, National Institute of Neurological Disorders and Stroke, National Institutes of Health, Bethesda, Maryland 20892;* [2]*Department of Pathology, Uniformed Services University of the Health Sciences, Bethesda, Maryland 20814*

KEY WORDS Mouse hepatitis virus, Remyelination, In situ hybridization, Oligodendrocyte

ABSTRACT C57Bl/6N mice develop a CNS demyelinating disease when inoculated intracranially at 4 weeks of age with the A59 strain of mouse hepatitis virus (MHV-A59). In order to explore the virus-host interactions, the histological features of the demyelinating disease were correlated with the spatial and temporal distribution of viral transcripts and the expression of oligodendrocyte-specific genes (myelin basic protein, proteolipid protein, myelin-associated glycoprotein, and 2′,3′cyclic nucleotide 3′-phosphohydrolase) in the spinal cord of diseased mice. Three distinct phases in the disease were identified. In the first phase, 1 week postinfection (1 WPI), virus replication was widespread in both gray and white matter but was preferentially occurring in glial cells. In the ventral and dorsal root zones where viral transcripts were most abundant, all myelin gene transcripts were decreased before demyelination was seen. During the second phase of the disease (2-3 WPI), viral transcripts decreased in abundance and became restricted to the white matter. Numerous demyelinating lesions were observed and were characterized by inflammatory cells, paucity of oligodendrocytes, and a profound decrease of all myelin gene transcripts. In the third phase of the disease (4-6 WPI) no viral transcripts were detected, and remyelination began. In the lesions and the tissue surrounding them, transcripts of all myelin genes increased to levels above normal. The increased expression of myelin gene transcripts occurred in a synchronized manner and with a cellular distribution reminiscent of that seen in developmental myelination. These molecular events correlated with efficient remyelination and clinical recovery in this murine demyelinating disease.

INTRODUCTION

In the central nervous system (CNS) myelin allows fast saltatory conduction of electrical signals to occur along ensheathed axons. Therefore, demyelination can cause important neurological dysfunction such as that seen in multiple sclerosis of man (reviewed in Silberberg, 1986). In some demyelinating diseases, myelin can be repaired, and clinical recovery occurs (reviewed in Ludwin, 1981). This indicates that glial cells involved in the myelination program are capable of reconstructing properly myelinated tracts in the diseased adult nervous system. While many aspects of the cellular and molecular events leading to myelination during development have been elucidated (reviewed in Lemke, 1988; Raff and Miller, 1984; Wood and Bunge, 1984), those underlying myelin repair in the adult CNS are poorly understood. Thus, a detailed analysis of the events during remyelination is needed and may lead to the discovery of methods to enhance myelin repair when it is insufficient.

In small rodents, several experimental demyelinating diseases have been described over the last two decades

Received January 11, 1989; accepted May 3, 1989.

Victor L. Friedrich, Jr., is now at Brookdale Center for Molecular Biology, Mt. Sinai Medical School, New York, NY 10029.

Catherine Godfraind is now at Service d'Anatomie Pathologique, Cliniques Universitaires Saint-luc, B-1200 Bruxelles, Belgium.

Address reprint requests to Dr. Craig Jordan, NIH/NINDS, Building 36, Room 5D04, Bethesda, MD 20892.

(reviewed in Ludwin, 1981). Those diseases that most closely resemble human demyelinating diseases such as multiple sclerosis fall into two groups. In the first group, a variety of myelin components can induce an autoimmune demyelinating disease such as experimental allergic encephalomyelitis (Raine, 1984; Tuohy et al., 1988). In the second group, different viruses can infect glial cells and cause CNS demyelination. Among the RNA viruses, a mouse picornavirus causes demyelination during Theiler's murine encephalomyelitis (Aubert et al., 1987; Chamorro et al., 1986; Lipton and Dal Canto, 1976). In this model, virus persists at the sites of the lesions although at low levels, and infected cells appear to survive for prolonged periods of time. In contrast, the JHM and A-59 strains of the coronavirus mouse hepatitis virus (MHV) usually cause an acute glial cell infection (Herndon et al., 1977; Knobler et al., 1981; Lavi et al., 1984a; Sorensen et al., 1981; Stohlman and Weiner, 1981; Woyciechowska et al., 1984). This infection may result in loss of oligodendrocytes and their myelin sheaths, sometimes with a subsequent autoimmune response to myelin antigens (Watanabe et al., 1983). Mice infected with the A59 strain of MHV have an initial acute phase of the disease accompanied by a vigorous immune response, which results in efficient clearing of the virus (Woyciechowska et al., 1984). Clinical recovery and myelin repair occur in the following 2–8 weeks (Kristensson et al., 1986; Lavi et al., 1984a,b; Woyciechowska et al., 1984). Although the viral-induced demyelinating lesions closely resemble those seen in multiple sclerosis, no specific association between multiple sclerosis and coronaviruses has been demonstrated so far (Fleming et al., 1988). We have chosen the MHV-A59 model for our studies since the virus caused demyelination in the spinal cord of a high proportion of the animals; subsequently, myelin repair can be followed closely in these spinal cord regions.

We have previously used in situ hybridization to analyze the expression of myelin genes in the spinal cord of both normal and diseased mice (Jordan et al., 1989, submitted; Kristensson et al., 1986). During active CNS myelination in the spinal cord white matter, we found high levels of transcripts for four myelin-specific genes: myelin basic protein (MBP), proteolipid protein (PLP), myelin-associated glycoprotein (MAG), and 2′,3′-cyclic nucleotide 3′-phosphohydrolase (CNP). In the case of MBP, a subset of transcript forms that appear during early development and contain exon 2 genetic information were highly expressed during myelination and sharply decreased thereafter (Jordan et al., 1989). We also examined MBP expression in the demyelinating animals and found that MBP transcripts were reduced in the lesions compared to the rest of the white matter (Kristensson et al., 1986). Later, MBP transcripts containing exon 2 information specifically increased in and around the lesions, before other MBP transcript forms or histological evidence of remyelination was detected (Jordan et al., submitted).

In the present study, we analyzed the spatial and temporal distribution of viral transcripts in the spinal cord tissue of diseased mice and correlated viral replication with the development of demyelinating lesions and the relative amounts of transcripts of four myelin genes. We then followed the expression of these four myelin gene transcripts during remyelination, using MBP as a reference. Three successive phases were identified in the course of the disease. During the first phase, virus replication was widespread and appeared to reduce myelin gene transcripts below normal levels. In the second phase, demyelinating lesions formed and showed a dramatic loss in myelin gene transcripts while the viral transcripts were progressively cleared. In the third phase, all myelin gene transcripts in and around the lesions increased above normal levels in a synchronized manner while remyelination proceeded.

MATERIALS AND METHODS

Viral Inoculation, Tissue Preparation, and Histological Stains

Four-week-old C57Bl/6N mice were injected intracranially (i.c.) with 1,000 plaque-forming units of MHV-A59 as described previously (Jordan et al., submitted) (Kristensson et al., 1986). Four to 7 days postinfection >75% of the mice developed clinical symptoms that often included hindlimb weakness or paresis. Mice without signs of neurologic disease were excluded from the experiment. At various times postinoculation, animals were anesthetized, perfused with 4% formaldehyde in 0.1 M phosphate buffer pH 7.4 (PB), and 2–3 mm slices of cervical spinal cords were frozen for 8–10 μm cryosectioning as described (Jordan et al., 1989). Adjacent sections from the same block of tissue were mounted on gelatin-coated slides and stored at −20°C for Sudan black staining, immunolabeling for various glial-specific proteins, or in situ hybridization (see below). The lipophilic dye Sudan black was used to stain myelin and therefore to identify the myelin lesions, as detailed previously (Jordan et al., submitted).

Other spinal cord tissue slices (1 mm) were postfixed with glutaraldehyde (1% in PB containing 5% sucrose) followed by osmium tetroxide (2% in the same buffer), dehydrated in graded ethanols, and embedded in epoxy resin. One-micron-thick sections were cut on an LKB Ultrotome III and counterstained with toluidine blue to study histologic features of the demyelinating lesions.

In a few instances, additional tissue was processed for 1 μm frozen sections following the technique of Tokuyasu (1973) and used for detection of viral transcripts by in situ hybridization. Transverse tissue slices (0.5–1 mm) of half spinal cord were postfixed overnight in 4% formaldehyde and then sequentially treated with 5%, 15%, 50%, and 2.3 M sucrose in phosphate-buffered saline (PBS) for 8–12 hours each before freezing by immersion in liquid nitrogen. One-micron transverse sections were cut at −90° C with glass knives on a Reichert-Jung ultracryotome (Ultracut E with FC4D

attachment). Sections were transferred in 2.3 M sucrose to gelatin-coated slides, fixed with 4% paraformaldehyde, processed for in situ hybridization, and counterstained with toluidine blue.

Immunofluorescence

For double label immunofluorescence, cryostat sections were permeabilized with 100% ethanol at −20° C for 15 min, transferred to room temperature and rinsed in PBS 2 × 3 minutes, 1% sodium borohydride in PBS for 5 minutes, rinsed in PBS 2 × 3 minutes, and equilibrated in 0.5 M Tris buffer pH 7.6 (TB). Sections were treated with blocking buffer (3% normal goat serum, 10% BSA, 0.1% gelatin, 0.05% sodium azide in TB) for 30 minutes then overnight at 4°C with a mixture of both primary antibodies in dilution buffer (1% BSA, 0.1% gelatin, and 0.05% sodium azide in TB) to which 0.1% biotin was added. The rat monoclonal 2.2B10.6 against glial fibrillary acidic protein (GFAP) was kindly provided by V. Lee (Lee et al., 1984). The rabbit anti-myelin basic protein (MBP) serum was raised against a synthetic peptide corresponding to the first 20 amino acids of human MBP and kindly provided by J. Kamholz et al. (1986). The sections were rinsed 3 × 20 min in TB at room temperature and then incubated with a mixture of sheep anti-rat antibody conjugated to biotin (Amersham) and goat anti-rabbit antibody conjugated to fluorescein (ICN Immunobiologicals) in dilution buffer for 1 hour. Following rinses in TB, the sections were incubated in streptavidin-conjugated rhodamine (Molecular Probes) for 1 hour. Finally, the tissue was postfixed with 4% paraformaldehyde in TB for 10 minutes, and coverslips were mounted with 80% glycerol in 0.5 M Tris pH 8.2 with 0.05% sodium azide. Specimens were viewed on a Zeiss Photomicroscope III equipped with the appropriate fluorescence filters.

In Situ Hybridization

Two different types of probes were used to detect the MHV-A59 transcripts. For one probe we used the clone g^2344 (Compton et al., 1987) derived from a clone of the MHV-A59 genome (kindly supplied by Dr. S. Weiss; Budzilowicz et al., 1985), which corresponds to 1800bp encompassing genes 5 and 6. To prepare a cRNA probe we linearized the clone g^2344 with Hind-III, performed in vitro transcription with T7 polymerase (Promega Biotec) and ^{35}S-UTP, and fragmented the labeled RNA by limited alkaline hydrolysis as described (Jordan et al., 1989). We also prepared two end-labeled (see below) synthetic oligonucleotide (48 nucleotides each) corresponding to the MHV-A59 nucleocapsid gene: oligonucleotide 388^- is complementary to nucleotides 388–435; and oligonucleotide 1444^- is complementary to nucleotides 1444–1491 following the numbering of Armstrong et al. (1983). Because the RNA transcripts of MHV are organized as nested sets that all contain the 3′ end of the genome, the oligonucleotide probes recognize all seven message species, and the cRNA probe recognizes six of the seven message species.

Synthetic oligonucleotide probes (48–50 nucleotides) specific for the myelin protein genes MBP, PLP, MAG, and CNP were chosen and 3′ end-labeled with ^{35}S-dATP to a specific activity of 2–3 × 10^8 cpm/μg as previously described (Jordan et al., 1989). Proximate spinal cord sections were hybridized with each of these probes at a concentration of 1–2 × 10^6 cpm per 50 μl following previously established conditions (Jordan et al., 1989). At least two mice were analyzed with each probe at each time point. The location of bound probe was visualized by direct apposition of the cryostat sections against Kodak X-OmatAR film or by coating the slides with Kodak NTB2 emulsion, developing, and counterstaining with cresyl violet (Jordan et al., 1989). Film and emulsion autoradiography were sometimes done sequentially on the same sections, but this required longer exposure times for the second procedure because of isotope decay. Actual exposure times are indicated in figure legends. Pseudocolor conversions of autoradiograms were generated on a Loats image analysis system.

RESULTS

We first examined the histological features of demyelination and remyelination in the spinal cord of infected mice that revealed the hallmarks of inflammatory demyelinating diseases as described earlier (Kristensson et al., 1986). Spinal cord white matter from normal mice is characterized by close packing of myelinated axons, with neuroglial cells interspersed between the axons (Fig. 1A). Foci of inflammation and demyelination developed within spinal cord white matter 6–10 days after intracranial inoculation with MHV-A59. Although asynchrony from lesion to lesion was observed, most lesions displayed a common pattern of initiation and progression. The earliest lesions, seen 1 and 2 weeks postinfection (WPI), exhibited collections of inflammatory cells within the subarachnoid space and nearby white matter (Fig. 1B), with minimal destruction of myelin. More advanced lesions, 3 WPI or later, showed partial or complete destruction of myelin sheaths, and were populated by debris-filled macrophages and other inflammatory cells (Fig. 1C). Oligodendrocytes, identified by light and electron microscopy, were reduced in number or virtually eliminated within these lesions, while axons remained largely intact. Evidence of CNS remyelination was occasionally seen 3–4 WPI by light microscopy and confirmed by electron microscopy (Figs. 1C, 2). Axons surrounded by a few loose turns of myelin or thin myelin sheaths were detectable after 3 WPI (Fig. 1C) and later became more common around the lesions where demyelination was well advanced (Fig. 2). Remyelination continued as demyelination subsided; by 12 WPI, lesions were well remyelinated (although myelin sheaths were thinner

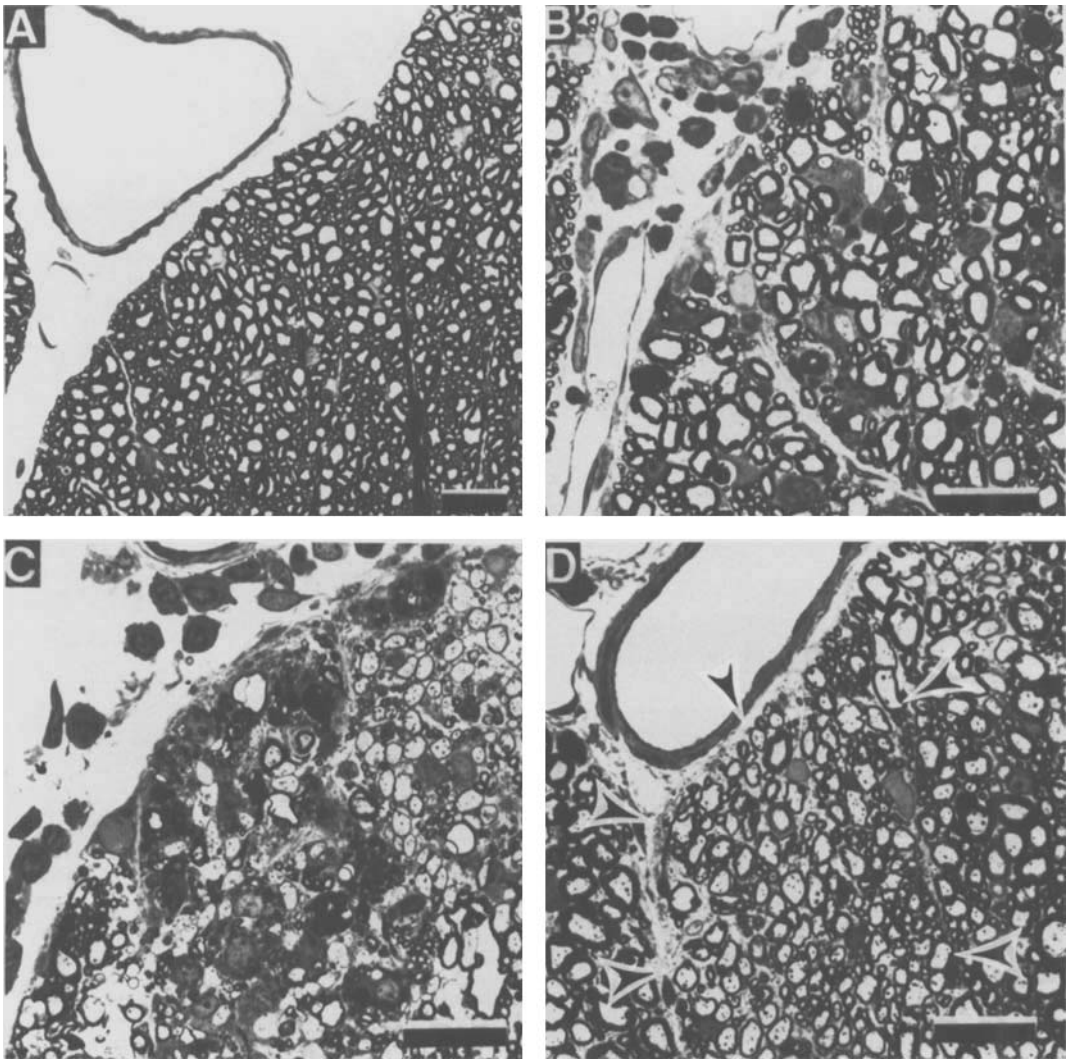

Fig. 1. Histological aspects of demyelinating and remyelinating lesions. One-micron epon sections of mouse cervical spinal cord were stained with toluidine blue. **A:** Control section with normal myelin sheaths and no cellular infiltrates. **B:** At 14 days postinfection (PI) some myelin sheaths are degenerating and cellular infiltrates are present. **C:** At 24 days PI, extensive myelin destruction is seen as well as cellular infiltrates and debris-laden macrophages. **D:** At 85 days PI, a large area of thinly remyelinated axons is seen (delineated by arrowheads), while normal thick myelin sheaths are present at the periphery. Bar, 20 μm.

than normal myelin sheaths), and cellular infiltrates had largely cleared from the white matter and subarachnoid space (Fig. 1D).

Expression of MHV-A59 Viral Transcripts in the Course of the Disease

We analyzed how the spatial and temporal distribution of viral transcripts correlated with histological changes in spinal cord of infected animals. Cervical spinal cord sections harvested 1, 2, 3, 4, and 12 WPI were hybridized with the ^{35}S-cRNA probe. Adjacent sections from the same blocks of tissue were stained for myelin with Sudan black to identify and localize demyelinated lesions. At 1 WPI, viral transcripts were very abundant both in white matter and gray matter and could clearly be seen in white matter areas, which were still well myelinated (Fig. 3A,E). The most frequently affected sites and those with the highest abundance of viral transcripts were in the dorsal and ventral root regions (Fig. 3E), where the first demyelinating lesions often appeared (Fig. 3A). At 2 WPI, large areas of demyelination were found (Fig. 3B), again mostly in ventral and dorsal root regions. At that time, viral transcripts were less abundant and were mostly cleared from the gray matter as well as from areas where demyelination was pronounced (compare Fig. 3B and F). Viral transcripts persisted only in white matter at 3 WPI (Fig. 3G), and by 4 WPI, they were either undetect-

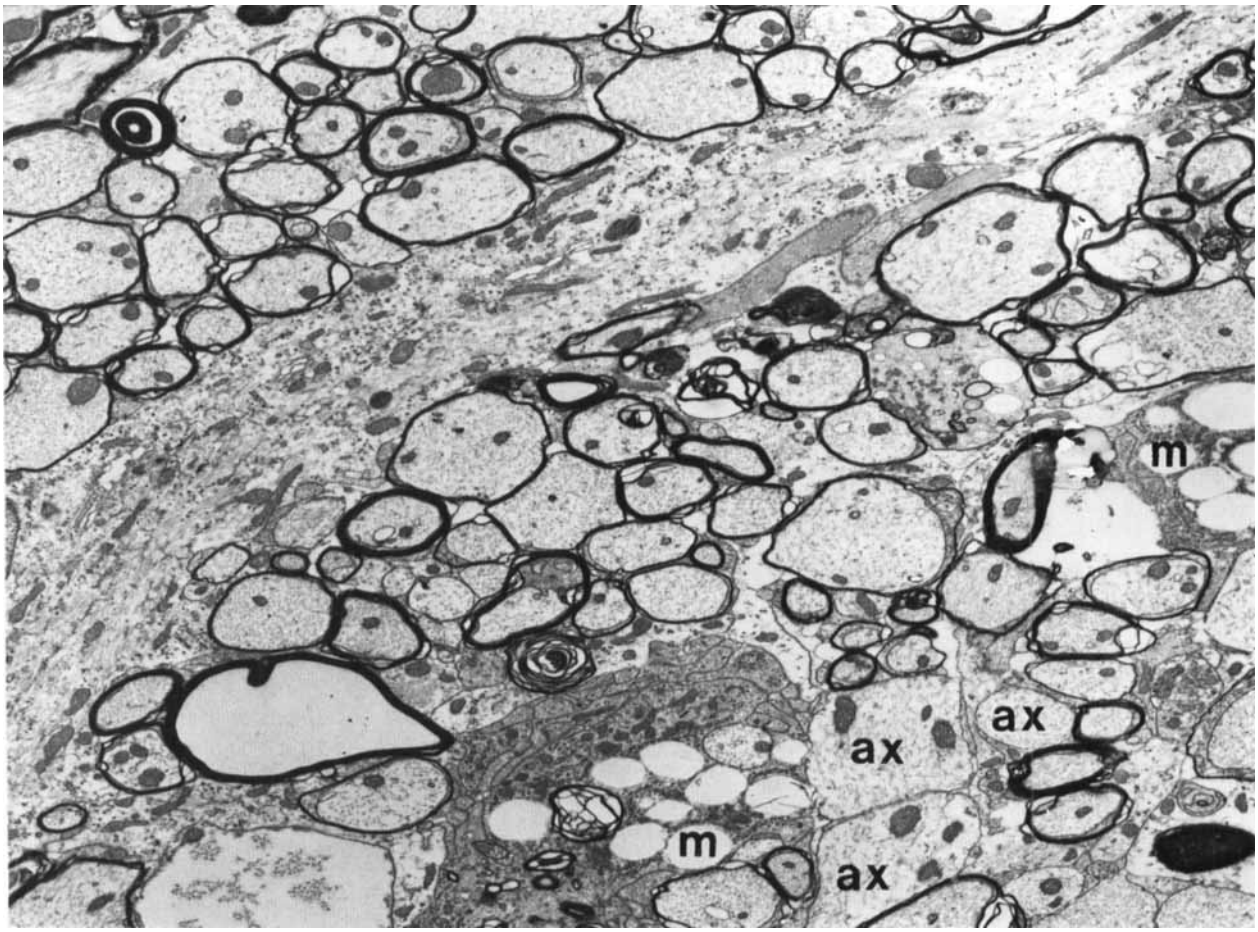

Fig. 2. Electron micrograph of a ventral root region from the cervical spinal cord at 4 WPI. Groups of axon fibers ensheathed with varying thicknesses of myelin are readily apparent on each side of a long astrocytic process crossing the field (nucleus on the left). A few completely demyelinated axons (ax) and nearby macrophages (m) are seen at the bottom of the picture. Scattered myelin debris is still present. The thinly myelinated axons are due to remyelination. In other micrographs, thinly myelinated axons were seen grouped around a young, light-staining oligodendrocyte and its processes.

able or limited to a few small foci (Fig. 3H) while large demyelinated lesions were seen in almost all sections (Fig. 3D). Occasionally lesions involved as much as 50% of the white matter. At 12 WPI, viral mRNA was not detected, and myelin appeared normal by Sudan black staining (data not shown) even though remyelinated sheaths were thinner than normal (Fig. 1D).

In order to identify more precisely the cell type with which viral transcripts were associated, we performed in situ hybridization on 1 μm frozen sections, from 1 WPI mice, using ^{35}S-labeled oligonucleotide probes. MHV-A59 transcripts were localized in clusters in the white matter (Fig. 3I) and in the gray matter (Fig. 3J). These clusters were clearly associated with individual cell bodies of glial cells but not with neurons (Fig. 3J). These findings substantiate that the virus replicates only in glial cells in vivo as well as in vitro (Dubois-Dalcq et al., 1982; Lavi et al., 1984a).

Loss of Myelin-Specific mRNAs Precedes Demyelination

It was intriguing that no substantial demyelination was seen at 1 WPI even though the viral mRNA was so abundant. Moreover, cresyl violet staining at 1 WPI did not reveal clear groups of inflammatory cells (Fig. 4B) although such cells did appear later in the disease. In an attempt to detect other changes induced by the infection, we examined the expression of MBP, a protein specific for oligodendrocytes. MBP antiserum stained myelinated fibers of white and gray matter in these 1 WPI tissues just as in normal animals (Fig. 4A).

We then investigated whether mRNAs specific for four myelin protein genes were present in normal amounts at 1 WPI. Sections from the same block of tissue were each hybridized with one of several ^{35}S-oligonucleotide probes for the myelin-specific mRNAs of

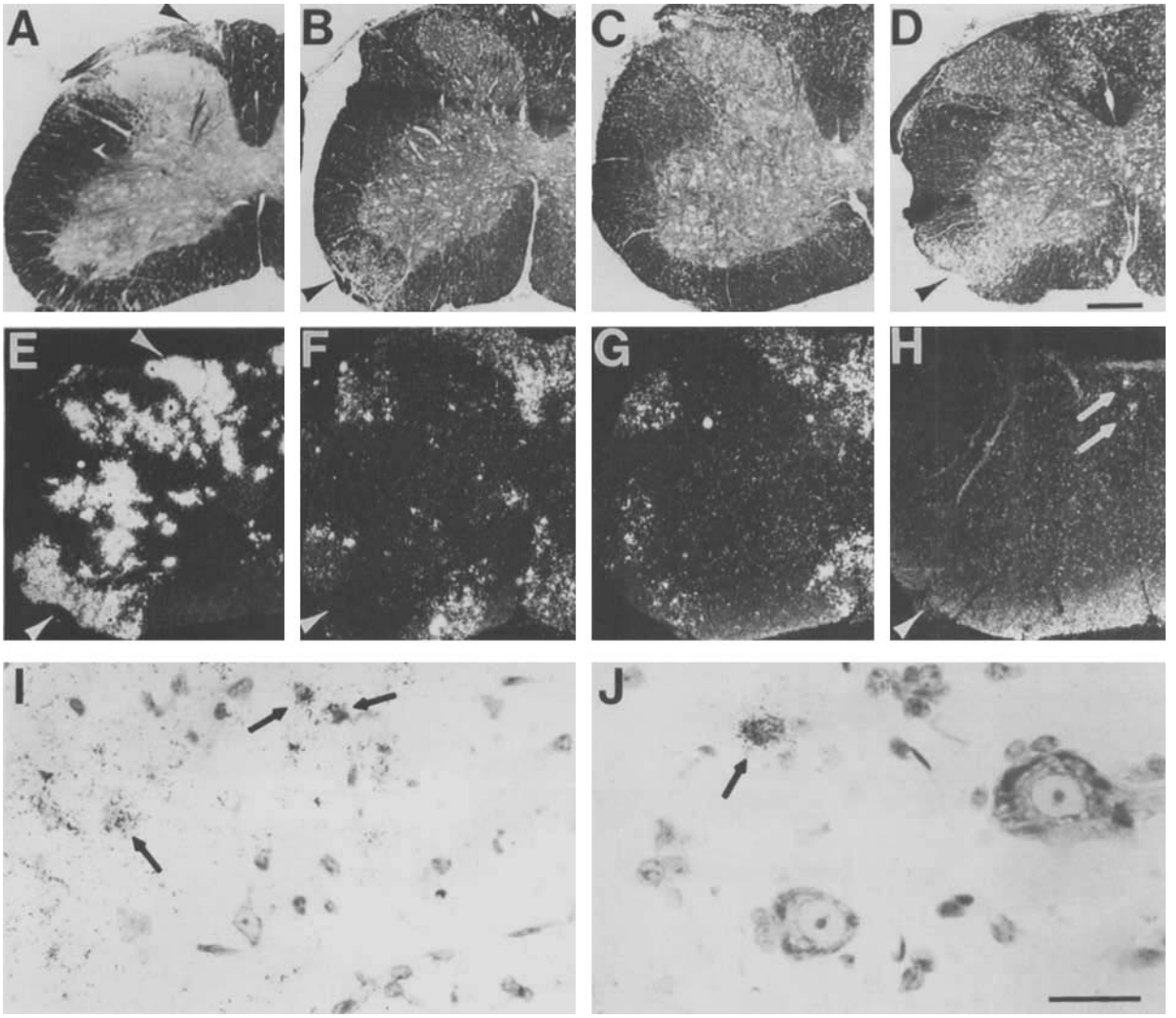

Fig. 3. Time sequence analysis of viral transcript expression and demyelination in the spinal cord. Eight to 10 μm cryostat sections (A–H) were either stained with Sudan black (A–D) or hybridized with the MHV-A59 cRNA probe (E–H, 8 day exposure) and viewed by darkfield microscopy. At 1 WPI, demyelination was rare and only in discrete regions (A, arrowhead), while viral transcripts were present in both gray and white matter regions; note abundance of transcripts at the dorsal and ventral root regions (E, arrowheads). At 2 and 3 WPI (B, F and C, G, respectively) the loss of myelin was detected, especially in the ventral root zone (arrowhead). Viral transcripts were less abundant and mostly restricted to the white matter where demyelinated lesions existed (arrowhead). The ventral root lesion in B has already been cleared of viral transcripts (F), while the same region in C and G still has viral transcripts but no apparent demyelination, illustrating the asynchrony of lesions. At 4 WPI, prominent areas of demyelination still existed (D, arrowhead), but viral transcripts had disappeared except for rare foci (H, arrows). I,J: Brightfield micrographs of 1 μm frozen sections (1 WPI), which were hybridized with the MHV oligonucleotide probes and exposed 24 days. MHV transcripts form clusters of grains which often associated with glial cell bodies (arrows) both in the white matter (I) and gray matter (J). Note that the large neurons are devoid of grains (J). Bar, 250 μm for A–H; 100 μm for I,J.

MBP, PLP, CNP, and MAG. We found that all four types of myelin-specific transcripts were reduced in the ventral root region 1 WPI (Fig. 4C–F). This myelin-specific transcript reduction correlated with, but was more restricted than, the location of MHV-A59 transcripts seen in nearby sections from the same blocks (Fig. 3E). The loss of myelin-specific transcripts occurred in the absence of obvious cellular infiltrates (Figs. 3A, 4B) and without detectable losses of MBP immunoreactivity or Sudan black-stained myelin lipids.

These results suggest that viral replication in oligodendrocytes reduces myelin gene transcripts before the onset of detectable demyelination. The most direct explanation would be that sick or dying oligodendrocytes stop producing mRNA but that the lipids and proteins of their myelin sheaths deteriorate and are cleared more slowly. Only after 2 WPI did we consistently observe loss of myelin protein and lipids and histological features of demyelination, in regions where myelin gene transcripts were reduced (see Figs. 1B,C, 3B).

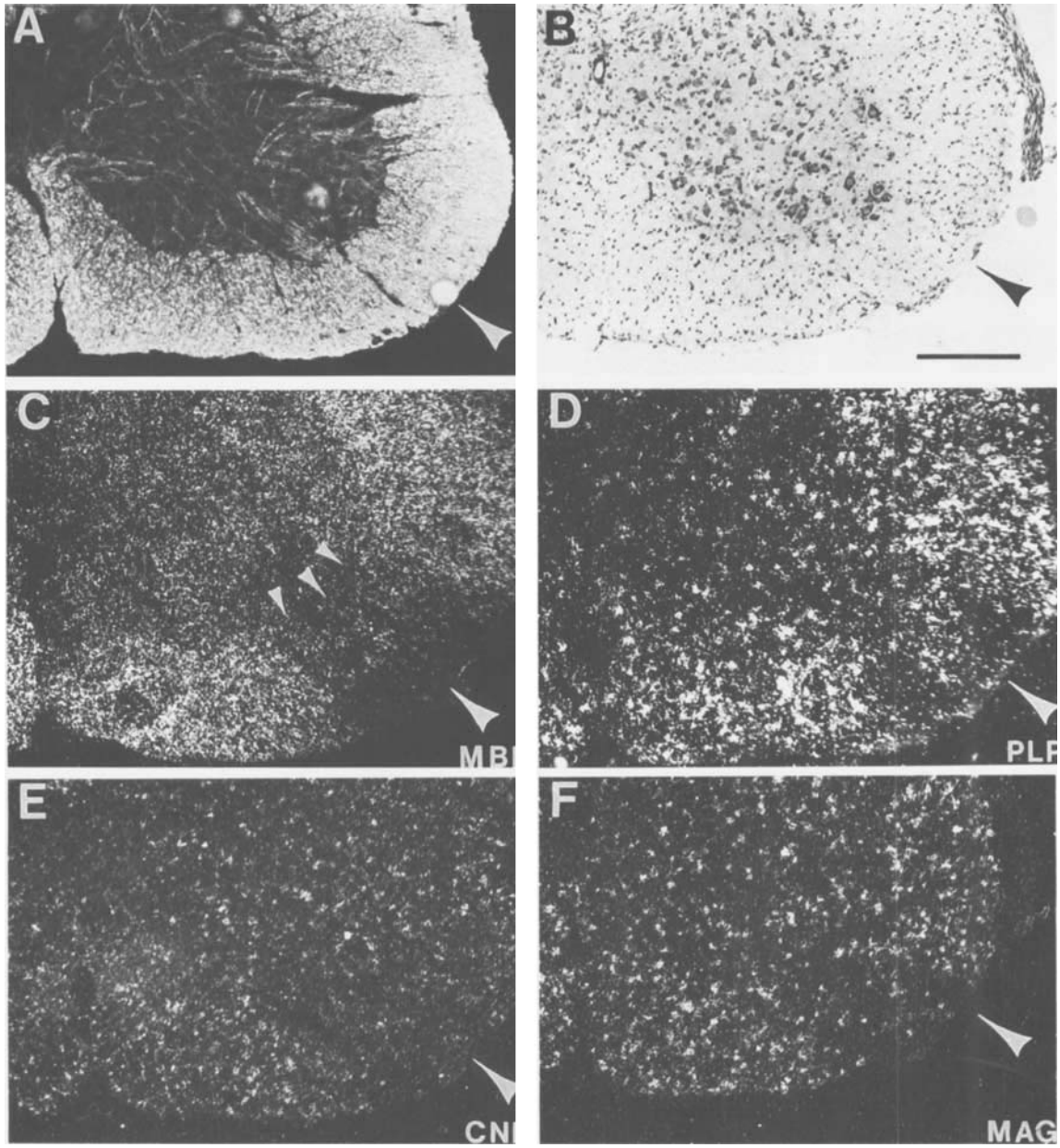

Fig. 4. Expression of myelin gene transcripts 1 WPI. Eight to 10 μm cervical spinal cord sections from the same block of tissue were immunostained for MBP (A), stained with cresyl violet (B), or probed by in situ hybridization for one of the myelin-specific transcripts (C–F). A: Antibody against myelin basic protein stained the myelinated fibers packed in the white matter and scattered in the gray matter. B: Cresyl violet staining revealed normal cell density in the white matter without clear cellular infiltrates at this time. C–F: In situ hybridization with probes for the transcripts of MBP, PLP, CNP, and MAG revealed a decreased expression in the ventral root region (arrowheads) when compared to other white matter regions in the same section. This tissue expressed high levels of viral transcripts in the ventral root lesion at this time, like those illustrated in Figure 2E. Specimens were photographed with fluorescence (A), brightfield (B), or darkfield (C–F) illumination. Emulsion dipped autoradiograms were exposed 10 days (C, D) or 34 days (E, F). Bar, 250 μm.

All Four Myelin Gene Transcripts Increase in and Around the Lesions During Remyelination

We have previously described an increase in MBP transcripts around the lesions at an early stage of remyelination (3½ to 4 WPI) (Kristensson et al., 1986) and found most recently that a subgroup of MBP transcripts containing exon 2 genetic information was preferentially increased at that time within the lesions (Jordan et al., submitted). We therefore examined how the expression of transcripts for other myelin genes correlated with myelin repair. Demyelinated areas could be identified at 5 and 6 WPI by the lack of MBP immunoreactivity (Fig. 5A), increased GFAP immuno-

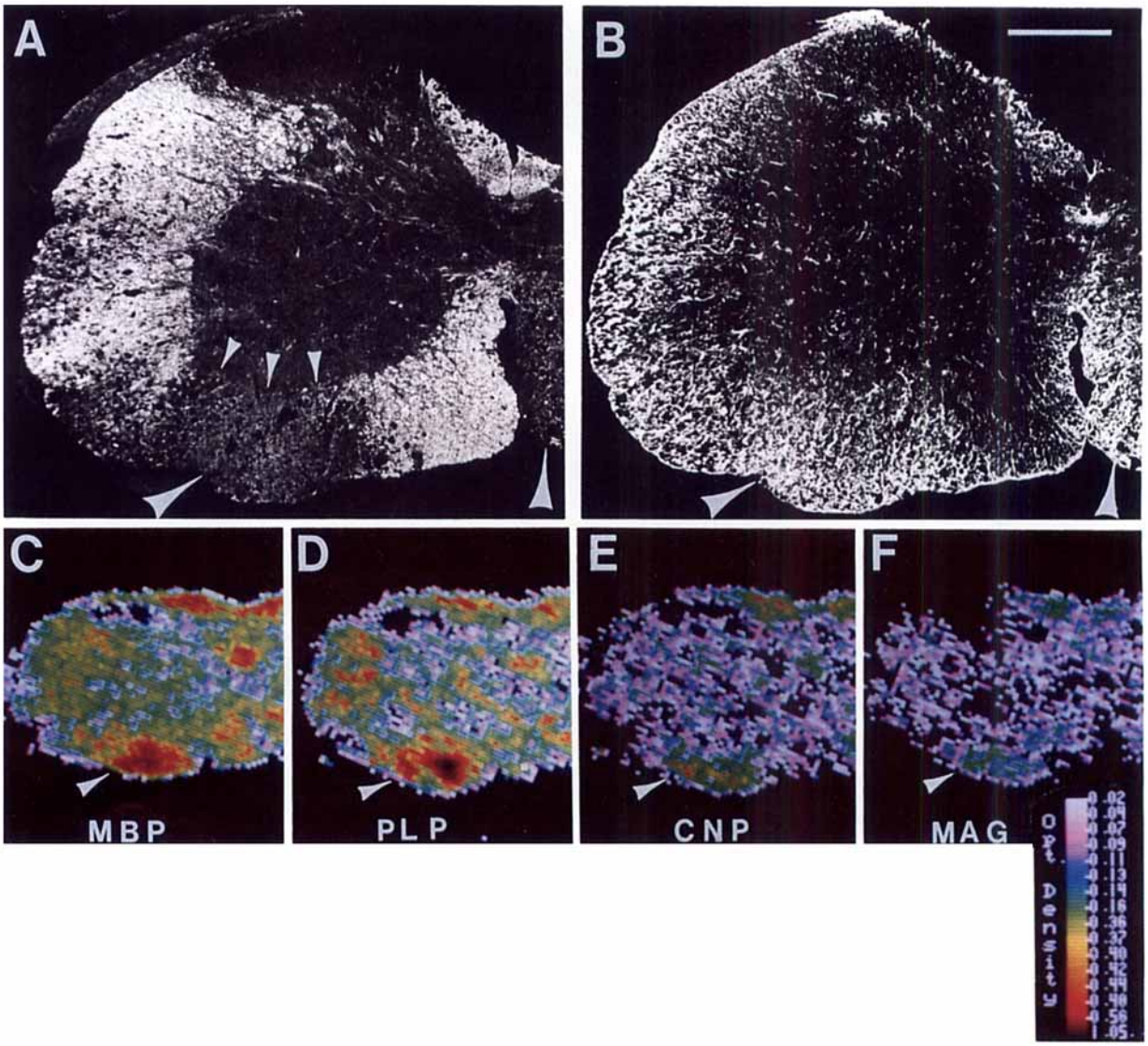

Fig. 5. Expression of myelin gene transcripts 5 WPI. Cryostat sections from a block of 5 WPI tissue were treated as in Figure 3. A: Myelin basic protein staining is considerably decreased in lesions (arrowheads). The largest lesion is located in the ventral root region. The ventral funiculus has a lesion on the right with a sharp boundary at the midline. The dorsal funiculus contains a lesion that is not visible in this partial section. B: The section in A was double-labeled and shows increased levels of GFAP within both ventral lesions (arrowheads). C–F: In situ hybridization with probes for MBP, PLP, CNP, and MAG, respectively; film autoradiograms were digitized and converted to pseudocolor. All genes have increased transcript levels in the large ventral root lesion (arrowheads); increases in message levels were also detected in the dorsal and ventral funiculus lesions. Film autoradiograms were exposed 5 days (C,D) or 26 days (E,F). Bar, 250 μm for A and B.

reactivity (Fig. 5B), reduced Sudan black staining (Fig. 6A), and by the presence of cellular infiltrates (Fig. 6B). At 5 WPI, these demyelinated areas showed a clear increase in all myelin gene transcript levels on film autoradiograms (Fig. 5C–F). All of the myelin gene transcripts were found to increase in lesions prior to detection of MBP by immunostaining. The most dramatic increases in the lesions were seen with MBP and PLP, while CNP and MAG transcripts were much less abundant, but still increased above normal levels (compare exposure times and optical density values of Fig. 5C and D with those in E and F). The relative abundance of these transcripts correlated well with the relative ratio of proteins in mature myelin (MBP, 30%; PLP 50%; CNP 5%, and MAG 1% of total myelin protein; Lees and Brostoff, 1984).

A relative increase in abundance of all myelin gene transcripts in and around the lesions was confirmed on emulsion autoradiograms at 6 WPI (Fig. 6). The differential cellular localization of MBP and PLP transcripts, described during developmental myelination (Jordan et al., 1989; Trapp et al., 1987), was also observed in the

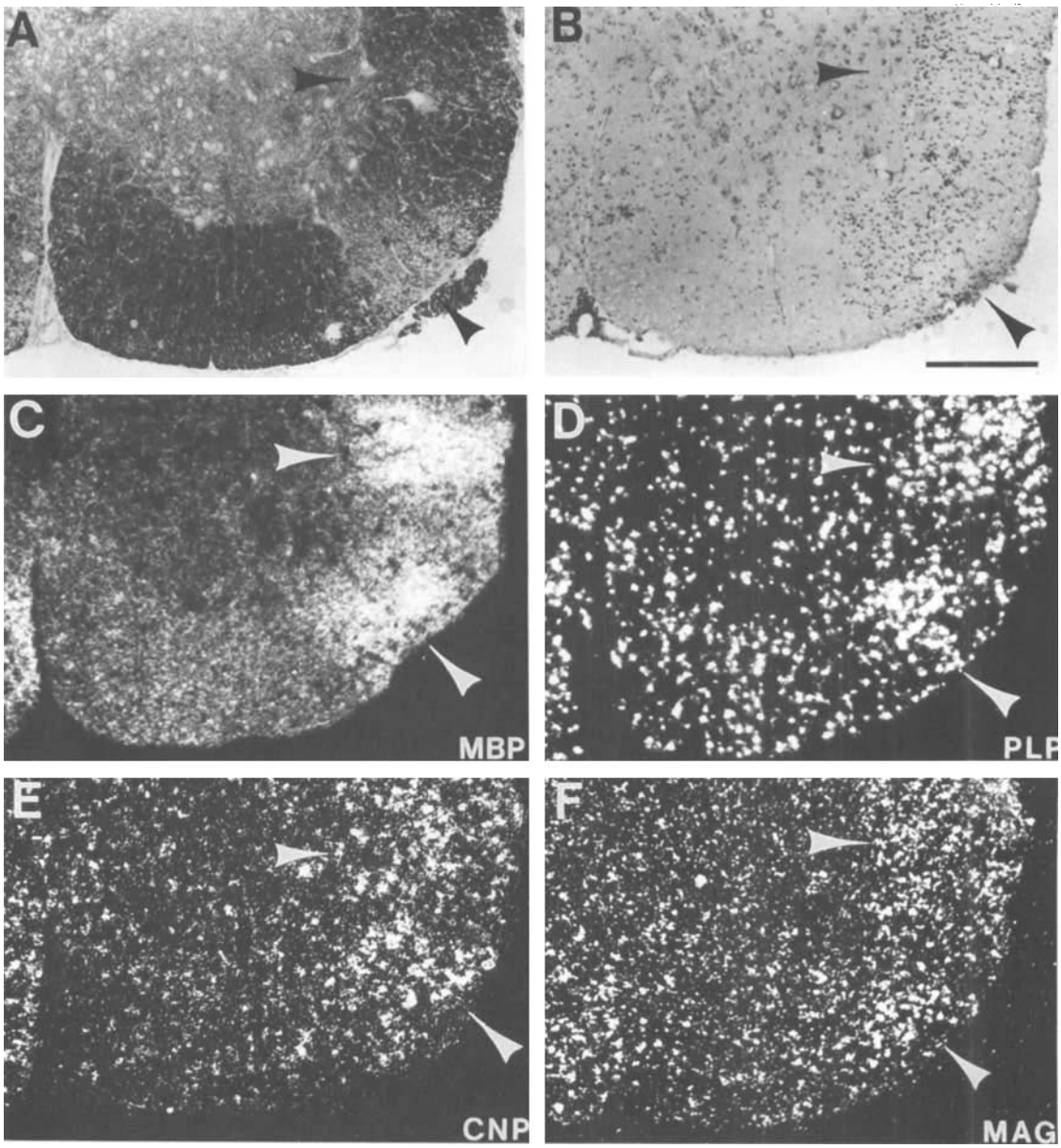

Fig. 6. Expression of myelin gene transcripts 6 WPI. Cryostat sections from a block of 6 WPI spinal cord were treated as in previous figures. A: Sudan black staining reveals a demyelinated lesion at the ventral root and a small lesion at the edge of the lateral column (arrowheads). B: Cellular infiltrates are present in and around the lesions (arrowheads) as revealed by cresyl violet staining. C–F: Autoradiograms from emulsion dipped sections after in situ hybridization with probes for MBP, PLP, CNP, and MAG, respectively. All transcript levels are increased in both lesions (arrowheads). The increased number of PLP, MAG, and CNP clusters within the lesions probably reflects an increased number of oligodendrocytes. Emulsion-dipped autoradiograms were exposed for 75 days. This long exposure was required because of isotope decay during previous film exposures of the same slides. Bar, 250 μm for A–F.

demyelinated areas with highest probe binding (Fig. 6C,D). PLP transcripts formed clusters (Fig. 6D) probably associated with individual oligodendrocyte cell bodies, while MBP transcripts were diffusely distributed in the areas of ongoing remyelination (Fig. 6C). This is likely related to the presence of transcripts in oligodendrocyte processes (Zeller et al., 1985). MAG and CNP transcripts formed less distinct clusters (Fig. 6E,F), resembling those observed during development (Jordan et al., 1989; Trapp et al., 1988).

At 12 WPI, remyelination had been progressing well for several weeks, but myelin sheaths were still thinner than normal (Fig. 1D). At this time we could not detect myelin lesions, viral transcripts, or cellular infiltrates; Sudan black staining and levels of myelin-specific transcript had returned to normal (data not shown).

DISCUSSION

In the present study, we followed the spread and clearing of a coronavirus (MHV-A59) in the mouse spinal cord by in situ hybridization and correlated this infection with the expression of oligodendrocyte-specific genes. We found that viral expression markedly reduced the levels of myelin gene transcripts at an early stage of the disease prior to demyelination (1 WPI). This reduction of myelin gene transcript levels persisted for several weeks and was associated with the development of histologic signs of demyelination and inflammation. This phase was followed by the coordinated reexpression of these myelin genes in and around the lesions where myelin repair occurred. It appears that in situ hybridization for specific gene transcripts can provide early and sensitive detection of both degenerative and repair processes in the central nervous system.

Our in situ hybridization analysis of viral expression confirms and extends previous observations on MHV-induced demyelination and remyelination (Lavi et al., 1984a,b; Perlman et al., 1988; Sorensen and Dales, 1985). MHV-JHM RNA was demonstrated in the CNS of mice inoculated intranasally at 10 days of age (Perlman et al., 1988). These mice developed a demyelinating encephalomyelitis, and the distribution of viral transcripts suggested viral spread along neuronal pathways and from contiguous structures. In our study, MHV-A59 appeared to replicate mostly in glial cells and not in neurons, even when the virus was present in the gray matter at 1 WPI. Similarly, virus was demonstrated by electron microscopy in oligodendrocytes infected with the JHM strain (Knobler et al., 1981; Powell and Lampert, 1975). Double-immunolabeling studies also showed MHV-A59 antigen in both oligodendrocytes and astrocytes at 1 WPI (C. Godfraind, unpublished observation). During the next 2 weeks, virus became restricted to white matter and was progressively cleared. This evolution correlates well with previous studies, which found that virus could not be isolated from the CNS after 2–3 WPI and that viral antigen could not be found in oligodendrocytes after 4 WPI (Lavi et al., 1984b; Woyciechowska et al., 1984). However, Lavi et al. (1984a) found occasional positive foci by in situ hybridization in a few animals at 10 months PI, suggesting that infection may sometimes persist and/or recur in older animals.

Although very few histological signs of demyelination were found at 1 WPI, a definite decrease of all myelin gene transcripts (MBP, PLP, MAG, and CNP) was observed in those white matter regions where viral transcripts were most abundant, the ventral and dorsal root regions. This early decrease in the expression of myelin genes was correlated with replication of virus in oligodendrocytes, but without a clear demonstration of reduced oligodendrocyte numbers. Thus active viral replication and a decrease in specific host cell gene expression are the hallmarks of the first phase of this disease. In the second phase of the disease (2–3 WPI), demyelinating lesions formed (in areas commonly supporting viral replication), and a dramatic loss of all myelin gene transcripts was observed in these lesions. The lesions were characterized by inflammatory cell infiltrates, macrophages phagocytosing cellular and myelin debris, and the lack of both Sudan black and MBP staining. In contrast, an increase in GFAP immunoreactivity in the lesions (Fig. 5B) and throughout the spinal cord was observed (Godfraind et al., 1988). The number of oligodendrocytes in the lesions was greatly reduced, an observation that correlates with the dramatic decrease in myelin gene transcripts and is likely due to virus-induced cell death.

In the third phase of the disease (at 4–6 WPI), demyelinated lesions still existed, while the first signs of myelin repair were also detected. The earliest sign of myelin repair at the molecular level was an increase in the subset of MBP transcripts containing exon 2 information. This increased expression was limited to scattered oligodendrocytes found in or near demyelinated lesions (Jordan et al., submitted). These transcripts are most abundant at the onset of myelination in developing animals and are reduced in adult animals when other MBP transcript forms predominate (de Ferra et al., in preparation) (Jordan et al., 1989; Kamholz et al., 1988). This sequential expression of MBP transcript subsets was also seen in lesions of MHV-infected mice undergoing remyelination (Jordan et al., submitted). In the present study, we showed that other myelin gene transcripts (MBP, PLP, MAG, and CNP) were also increased in the lesions and in the surrounding tissue and were expressed synchronously as in developmental myelination (Jordan et al., 1989). This is reminiscent of immunocytochemical observations on the superior cerebellar peduncle of animals demyelinated with cuprizone, where expression of myelin proteins in remyelinating oligodendrocytes appears to revert to that seen during normal development (Ludwin and Sternberger, 1984). Thus, the coordinated and timely expression of myelin genes observed in vivo and in vitro during development (Dubois-Dalcq et al., 1986; Kanfer et al., 1989; Monge et al., 1986; among others) may also be characteristic of remyelination in the adult CNS.

As in developing white matter, MBP transcripts in infected animals showed a diffuse distribution, while PLP transcripts were concentrated in the cell body of oligodendrocytes (Jordan et al., 1989; Trapp et al., 1987). Because PLP transcripts were clustered, one could observe that increased numbers of oligodendrocytes were present in and around the lesions when compared to the normal white matter regions. This observation correlates with evidence that new oligodendrocytes were generated in the spinal cords of these infected animals (Armstrong et al., 1988; Godfraind et al., 1988). Surviving oligodendrocytes around lesions may also increase the synthesis of myelin gene transcripts and send additional processes to myelinate neighboring naked axons.

In the model we have investigated, viral infection

resulted in demyelination, which was followed by remyelination. Our results demonstrated dramatic changes in viral and myelin gene transcript levels that were characteristic for each stage of this process. This study, together with our previous analysis of MBP gene expression (Jordan et al., submitted; Kristensson et al., 1986), clearly showed that reexpression of myelin genes during CNS remyelination follows a program reminiscent of that observed during developmental myelination.

ACKNOWLEDGMENTS

We would like to thank Dr. S. Young for the use of the Loats image analysis system and R. Rusten and S. Wetherell for excellent technical assistance. We would also like to acknowledge the gift of antibodies by Drs. V. Lee and J. Kamholz. This study was supported in part by NIH grant AI18997 and grant R07403 from the Uniformed Services University of the Health Sciences. The opinions or assertions contained herein are the private views of the authors and are not to be construed as official or reflecting the views of the Department of Defense or the Uniformed Services University of the Health Sciences.

REFERENCES

Armstrong, R., Friedrich, V.L., Jr., Holmes, K.V., and Dubois-Dalcq, M. (1988) *In vitro* analysis of neuroglial cells isolated during demyelination and remyelination. *Soc. Neurosci. Abstr.*, 14:787.

Armstrong, J., Smeekens, S., and Rottier, P. (1983) Sequence of the nucleicapsid gene from murine coronavirus MHV-A59. *Nucleic Acids Res.*, 11:883–891.

Aubert, C., Chamorro, M., and Brahic, M. (1987) Identification of Theiler's virus infected cells in the central nervous system of the mouse during demyelinating disease. *Microbial Pathogenesis*, 3:319–326.

Budzilowicz, C.J., Wilczynski, S.P., and Weiss, S.R. (1985) Three intergenic regions of coronavirus mouse hepatitis virus strain A59 genome RNA contain a common nucleotide sequence that is homologous to the 3′ end of the viral mRNA leader sequence. *J. Virol.*, 53:834–840.

Chamorro, M., Aubert, C., and Brahic, M. (1986) Demyelinating lesions due to Theiler's virus are associated with ongoing central nervous system infection. *J. Virol.*, 57:992–997.

Compton, S.R., Rogers, D.B., Holmes, K.V., Fertsch, D., Remenick, J., and McGowan, J.J. (1987) *In vitro* replication of mouse hepatitis virus strain A59. *J. Virol.*, 61:1814–1820.

Dubois-Dalcq, M., Behar, T., Hudson, L., and Lazzarini, R.A. (1986) Emergence of three myelin proteins in oligodendrocytes cultured without neurons. *J. Cell Biol.*, 102:384–392.

Dubois-Dalcq, M., Holmes, K.V., Doller, E.W., and Haspel, M.V. (1982) Cell tropism and expression of mouse hepatitis virus (MHV) in mouse spinal cord cultures. *Virology*, 119:317–331.

Fleming, J.O., El Zaatari, F.A.K., Gilmore, W., Berne, J.D., Burks, J.S., Stohlman, S.A., Tourtellotte, W.W., and Weiner, L.P. (1988) Antigenic assessment of Coronaviruses isolated from patients with multiple sclerosis. *Arch. Neurol.*, 45:629–633.

Godfraind, C., Friedrich, V.L., Jr., Jordan, C.A., Holmes, K.V., and Dubois-Dalcq, M. (1988) Glial cell plasticity and remyelination following A59 mouse hepatitis virus induced demyelination. *J. Cell. Biochem. Abstr. [Suppl]*, 12C:p34.

Herndon, R.M., Price, D.L., and Weiner, L.P. (1977) Regeneration of oligodendroglia during recovery from demyelinating disease. *Science*, 195:693, 694.

Jordan, C., Friedrich, V., Jr., Dubois-Dalcq, M. (1989) In situ hybridization analysis of myelin gene transcripts in developing mouse spinal cord. *J. Neurosci.*, 9:248–257.

Kamholz, J., de Ferra, F., Puckett, C., and Lazzarini, R. (1986) Identification of three forms of human myelin basic protein by cDNA cloning. *Proc. Natl. Acad. Sci. U.S.A.*, 83;4962–4966.

Kamholz, J., Toffenetti, J., and Lazzarini, R.A. (1988) Organization and expression of the human myelin basic protein gene. *J. Neurosci. Res.*, 21:62–70.

Kanfer, J., Parenty, M., Goujet-Zalc, C., Monge, M., Bernier, L., Campagnoni, A.T., Dautigny, A., and Zalc, B. (1989) Developmental expression of myelin proteolipid, basic protein, and 2′,3′-cyclic nucleotide 3′-phosphodiesterase transcripts in different rat brain regions. *J. Mol. Neurosci.*, 1:39–46.

Knobler, R.L., Dubois-Dalcq, M., Haspel, M.V., Claysmith, A.P., Lampert, P.W., and Oldstone, M.B.A. (1981) Selective localization of wild type and mutant mouse hepatitis virus (JHM strain) antigens in CNS tissue by fluorescence, light and electron microscopy. *J. Neuroimmunol.*, 1:81–92.

Kristensson, K., Holmes, K.V., Duchala, C.S., Zeller, N.K., Lazzarini, R.A., and Dubois-Dalcq, M. (1986) Increased levels of myelin basic protein transcripts in virus-induced demyelination. *Nature*, 322:544–547.

Lavi, E., Gilden, D.H., Highkin, M.K., and Weiss, S.R. (1984a) Persistence of mouse hepatitis virus A59 RNA in a slow virus demyelinating infection in mice as detected by *in situ* hybridization. *J. Virol.*, 51:563–566.

Lavi, E., Gilden, D.H., Wroblewska, Z., Rorke, L.B., and Weiss, S.R. (1984b) Experimental demyelination produced by the A-59 strain of mouse hepatitis virus. *Neurology*, 34:597–603.

Lee, V.M.-Y., Page, C.D., Wu, H.-L., and Schlaepfer, W.W. (1984) Monoclonal antibodies to gel-excised glial filament protein and their reactivities with other intermediate filament proteins. *J. Neurochem.*, 42:25–32.

Lees, M.B. and Brostoff, S.W. (1984) Proteins of myelin. In: *Myelin*, P. Morell, ed. Plenum Press, New York, pp. 197–224.

Lemke, G. (1988) Unwrapping the genes of myelin. *Neuron*, 1:535–543.

Lipton, H.L. and Dal Canto, M.C. (1976) Theiler's virus induced demyelination: Prevention by immunosuppression. *Science*, 192:62–64.

Ludwin, S.K. (1981) Pathology of demyelination and remyelination. In: *Advances in Neurology: Demyelinating Diseases, Vol. 31*. S.G. Waxman and J.M. Ritchie, eds. Raven Press, New York, pp. 123–168.

Ludwin, S.K. and Sternberger, N.H. (1984) An immunohistochemical study of myelin proteins during remyelination in the central nervous system. *Acta Neuropathol. (Berl.,)* 63:240–248.

Monge, M., Kadiisky, D., Jacque, C., and Zalc, B. (1986) Oligodendroglial expression and deposition of four major myelin constituents in the myelin sheath during development: An *in vivo* study. *Dev. Neurosci.*, 8:222–235.

Perlman, S., Jacobsen, G., and Moore, S. (1988) Regional localization of virus in the central nervous system of mice persistently infected with murine coronavirus JHM. *Virology*, 166:328–338.

Powell, H.C. and Lampert, P.W. (1975) Oligodendrocytes and their myelin-plasma membrane connections in JHM mouse hepatitis virus encephalomyelitis. *Lab. Invest.*, 33:440–445.

Raff, M.C. and Miller, R.H. (1984) Glial cell development in the rat optic nerve. *Trends Neurosci.*, 7:469–472.

Raine, C.S. (1984) Biology of disease: The analysis of autoimmune demyelination: Its impact on multiple sclerosis. *Lab. Invest.*, 50:608.

Silberberg, D.H. (1986) Pathogenesis of demyelination. In: *Multiple Sclerosis*. W.I. McDonald and D.H. Silberberg, eds. Butterworth & Co., London, pp. 99–111.

Sorensen, O., Coulter-Mackie, M., Percy, D., and Dales, S. (1981) In vivo and in vitro models of demyelinating diseases. *Adv. Exp. Med. Biol.*, 142:271–286.

Sorensen, O. and Dales, S. (1985) *In vivo* and *in vitro* models of demyelinating disease: JHM virus in the rat central nervous system localized by *in situ* cDNA hybridization and immunofluorescent microscopy. *J. Virol.*, 56:434–438.

Stohlman, S.A. and Weiner, L.P. (1981) Chronic central nervous system demyelination in mice after JHM virus infection. *Neurology*, 31:38–44.

Tokuyasu, K.T. (1973) A technique for ultramicrotomy of cell suspensions and tissues. *J. Cell Biol.*, 57:551–565.

Trapp, B.D., Bernier, L., Andrews, S.B., and Colman, D.R. (1988) Cellular and subcellular distribution of 2′,3′-cyclic nucleotide 3′-phosphodiesterase and its mRNA in the rat central nervous system. *J. Neurochem.*, 51:859–868.

Trapp, B.D., Moeuch, T., Pulley, M., Barbosa, E., Tennekoon, G., and Griffith, J. (1987) Spatial segregation of mRNA encoding myelin-specific proteins. *Proc. Natl. Acad. Sci. U.S.A.*, 84:7773–7777.

Tuohy, V.K., Sobel, R.A., and Lees, M.B. (1988) Myelin proteolipid protein-induced experimental allergic encephalomyelitis: Variations of disease expression in different strains of mice. *J. Immunol.*, 140:1868–1873.

Watanabe, R., Wege, H., and ter Meulen, V. (1983) Adoptive transfer of EAE-like lesions from rats with coronavirus induced demyelinating encephalomyelitis. *Nature,* 305:150–153.

Wood, P.M. and Bunge, R.P. (1984) The biology of the oligodendrocyte. In: *Oligodendroglia.* W.T. Norton, ed. Plenum Press, New York, pp. 1–46.

Woyciechowska, J.L., Trapp, B.D., Patrick, D.H., Shekarchi, I.C., Leinikki, P.O., Sever, J.L., and Holmes, K.V. (1984) Acute and subacute demyelination induced by mouse hepatitis virus strain A59 in C3H mice. *J. Exp. Pathol.,* 1:295–306.

Zeller, N.K., Behar, T.N., Dubois-Dalcq, M.E., and Lazzarini, R.A. (1985) The timely expression of myelin basic protein gene in cultured rat brain oligodendrocytes is independent of continuous neuronal influences. *J. Neurosci.,* 5:2955–2962.